Colloids and Surfaces A: Physicochem. Eng. Aspects 506 (2016) 747–755

Contents lists available at ScienceDirect

Colloids and Surfaces A: Physicochemical and Engineering Aspects

journal homepage: www.elsevier.com/locate/colsurfa

Graphene oxide-based Fe_2O_3 hybrid enzyme mimetic with enhanced peroxidase and catalase-like activities

Lina Song[a,1], Chao Huang[b,1], Wei Zhang[a], Ming Ma[a], Zhongwen Chen[a], Ning Gu[a,*], Yu Zhang[a,*]

[a] State Key Laboratory of Bioelectronics, Jiangsu Key Laboratory for Biomaterials and Devices, School of Biological Science and Medical Engineering & Collaborative Innovation Center of Suzhou Nano Science and Technology, Southeast University, Nanjing 210096, PR China
[b] Institute of Pathogenic Microbiology, Jiangsu Provincial Center for Disease Control and Prevention, Nanjing 210009, PR China

HIGHLIGHTS

- A simple method to prepare GO-Fe_2O_3 hybrids was developed.
- The enzyme mimetic activity of Fe_2O_3 nanoparticles was effectively improved by simply introducing GO to form GO-Fe_2O_3 hybrids.
- The GO-Fe_2O_3 hybrids act as a pH-dependent dual-enzyme.
- GO-Fe_2O_3 hybrids exhibit the ability to degrade Rhodamine B.

GRAPHICAL ABSTRACT

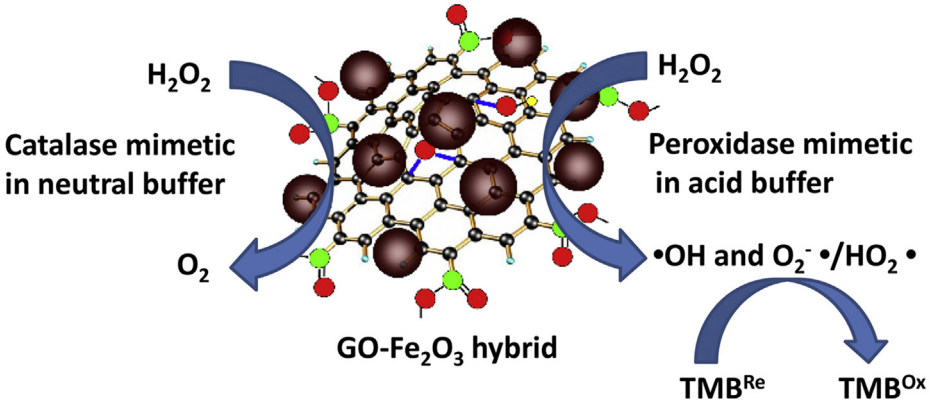

ARTICLE INFO

Article history:
Received 21 March 2016
Received in revised form 7 July 2016
Accepted 19 July 2016
Available online 25 July 2016

Keywords:
Graphene oxides
Fe_2O_3 nanoparticles
Hybrids
Peroxidase
Catalase

ABSTRACT

Graphene based materials are widely used in energy conversation and catalytic reaction due to their rapid electron transfer capacity and large surface area. Herein, graphene Fe_2O_3 (GO-Fe_2O_3) hybrids with enhanced peroxidase-like activity were fabricated. Enhanced peroxidase-like activity strongly depending on pH, temperature and hybrid concentration was observed and the peroxidase-like behavior fits well the Michaelis-Menten kinetic model. Free radicals, such as •OH and O_2^{-}•, as intermediates in the hybrid-H_2O_2 reaction system were directly demonstrated by electron spin resonance (ESR) technique and the selective radical inhibition experiments. Furthermore, it was found that the addition of TMB rapidly consumed •OH and O_2^{-}•, and subsequently leaded to the formation of blue TMB radical confirmed by the ESR and absorption spectroscopy. Besides acting as mimetic peroxidase in acidic buffer, the GO-Fe_2O_3 hybrids also displayed the enhanced catalase-like activity in neutral and alkaline buffers compared with individual Fe_2O_3 nanoparticles and GO sheet, respectively. The H_2O_2 decomposition catalyzed by the hybrids was demonstrated by ESR and the generated O_2 was measured using the dissolved oxygen electrode. All the results above demonstrate that the GO-Fe_2O_3 hybrids are a kind of effective pH-dependent mimetic dual-enzyme.

* Corresponding authors at: School of Biological Science and Medical Engineering, Southeast University, PR China.
E-mail addresses: guning@seu.edu.cn (N. Gu), zhangyu@seu.edu.cn (Y. Zhang).

[1] These authors contributed equally to this work.

http://dx.doi.org/10.1016/j.colsurfa.2016.07.037
0927-7757/

1. Introduction

Magnetic iron oxide nanoparticles have widely biomedical applications including protein immobilization and separation [1–3], magnetic targeting and drug delivery [4–6], cancer hyperthermia [7,8], magnetic resonance imaging (MRI) [9–12] and so on. Recently, it was also reported that Fe_3O_4 nanoparticles possess intrinsic enzyme mimetic activity and the mechanism may follow the Fenton reaction [13] written as (1) and (2), where k_1 and k_2 are the reaction rate constants.

$$Fe^{2+} + H_2O_2 \xrightarrow{k_1} Fe^{3+} + {}^{\bullet}OH + OH^- \quad k_1 = 76\left(\text{mol/L}\right)^{-1}\text{s}^{-1} \tag{1}$$

$$Fe^{3+} + H_2O_2 \xrightarrow{k_2} Fe^{2+} + {}^{\bullet}OOH + H^+ \quad k_2 = 0.002\left(\text{mol/L}\right)^{-1}\text{s}^{-1} \tag{2}$$

This surprising finding makes magnetic Fe_3O_4 nanoparticles a powerful analytic tool to simultaneously realize capture, separation and detection for the immunoassay of hepatitis B virus surface antigen (preS1), cardiac troponin I(TnI) [14], Carcino embryonic antigen (CEA), α-fetoprotein (AFP) [15], mouse IgG [16] and so on. However, Fe_3O_4 nanoparticles intended to be oxidized to Fe_2O_3 nanoparticles in the air [17], thus leaded to the instability of their enzyme-like activity. In addition, Fe_2O_3 nanoparticles possess weaker catalytic activity due to lacking of Fe^{2+} and low k_2 constant. To enhance the enzyme-like activity of Fe_2O_3 nanoparticles, modifying iron oxides with other materials such as Prussian blue is a practicable method. GO-Fe_2O_3 hydrides used as enzyme catalysts have been reported [18,19]. Likely, graphene materials could also be selected as a good candidate due to its unique properties. Qu [20] first discovered that Graphene oxide (GO) itself possesses peroxidase-like activity attributed to its rapid electron transfer and substrate adsorption capacities, but the peroxidase-like activity is very low because of the absence of reactive center like natural peroxidases. As we know, graphene-based materials of high strength [21], rapid carrier mobility [22,23] and excellent thermal conductivity [24] exhibit great potential in catalytic reaction and energy conversion [25]. When combined with graphene, many other materials showed enhanced catalysis and energy conversion ability. For example, reduced graphene oxides-TiO_2 nanoparticles (RGO-TiO_2) composites performed well in solar cells and photocatalytic applications [26]; Pt nanoparticles-functionalized graphene sheets (Pt-FGS) showed a higher electrochemical surface area and oxygen reduction activity with improved stability as compared with the commercial catalysts [27]. Magnetically separable $ZnFe_2O_4$-Graphene exhibits high photocatalytic performance under visible light irradiation [28]. Hence, designing hybrid assemblies containing enzyme-like nanoparticles based on graphene materials is an effective method to enhance the enzyme activity because of graphene materials' special structure and excellent properties, such as one-atom thickness, sp^2 hybridization, large surface area and rapid electron transfer capacity.

Herein we report that the enzyme mimetic activity of Fe_2O_3 nanoparticles can be effectively improved by simply introducing GO to form GO-Fe_2O_3 hybrids. We found the hybrid catalyst not only possesses peroxidase-like activity in an acid buffer but also shows catalase-like activity in neutral and alkaline environments, which suggests the hybrids can act as a pH-dependent dual-enzyme. The enzyme mimetic activity fits well with Michaelis-Menten equation and the hybrids exhibit much better catalytic ability than Fe_2O_3 nanoparticles or GO alone. Furtherly, we demonstrated the peroxidase and catalase-like activity of GO-Fe_2O_3 hybrids via directly and indirectly measuring end product formation and reaction intermedia using electron spin resonance and dissolved oxygen detection, and a possible reaction mechanism was proposed. The catalytic degradation of Rhodamine B (RhB) by GO-Fe_2O_3 hybrids with different reaction time, pH, temperature, H_2O_2 and hybrids concentration was investigated.

2. Experimental section

2.1. Materials

All chemicals used in this experiment were of analytical reagent grade. Graphene oxides (GO) was from Liu's research group of Suzhou University prepared according to previous reports [29–31]. Fe_2O_3@APTES nanoparticles were synthesized according to our group's previous literature [32,33]. 3,3′,5,5′-tetramethylbenzidine (TMB), 5,5′-dimethyl-1-pirroline-*N*-oxide (DMPO) and 2,2′-Azino-di (3-ethylbenzthiazoline-6-sulfonic acid (ABTS) were bought from Sigma Aldrich Co. Ltd. (3-aminopropyl) triethoxysilane (APTES) was purchased from Alfa Aesar Co. Ltd. Dimethyl sulfoxide (DMSO), glacial acetic acid (HAc), anhydrous sodium acetate (NaAc) were purchased from Sinopharm Chemical Reagent Co. Ltd. Hydrogen peroxide (30%) was obtained from Aladdin Co. Ltd. Dipotassium hydrogen phosphate, sodium phosphate dibasic, sodium chloride, and tetramethyl ammonium hydroxide were reagents from Shanghai Lingfeng Chemical Reagent Co. Ltd. Deionized water was used throughout the study.

2.2. Synthesis of GO-Fe_2O_3 hybrids

The Fe_3O_4 nanoparticles were prepared via the coprecipitation method and then Fe_2O_3 nanoparticles were obtained at 90 °C using O_2 as oxidizing agents. (3-aminopropyl) triethoxysilane (APTES) were coated on the surface of Fe_2O_3 nanoparticles according to literature [32,33]. The concentration of Fe_2O_3 nanoparticles solution was adjusting to 1.5 mg/mL. The Graphene oxides (GO) solution (6.8 mg/mL, 1 mL) were ultrasonicated for 1 h to form monolayer GO film. Then different amount of Fe_2O_3 nanoparticles aqueous solution were added to the monolayer GO solution with further ultrasonication for 2 h. The composite reaction was lasted for another 3.5 h on the thermostatic oscillator at 35 °C and 200 rpm to prepare GO-Fe_2O_3 hybrids. The purified precipitate by magnetic separation was GO-Fe_2O_3 hybrids and they were kept under 4 °C for later experiments.

2.3. Test of peroxidase-like activity of GO-Fe_2O_3 hybrids

The catalytic reaction was carried out in the anhydrous sodium acetate-glacial acetic acid (NaAc-HAc) buffer (0.2 M, pH 3.6) with 0.622 mM TMB (or 0.396 mM ABTS) and 852 mM hydrogen peroxide as substrates, and using GO-Fe_2O_3 hybrids as enzyme mimetics. The absorbance values (Abs) of the reaction system catalyzed by GO-Fe_2O_3 hybrids, Fe_2O_3 nanoparticles and GO were recorded for 60 min with the microplate reader for comparing their activities.

2.4. Test of catalase-like activity of GO-Fe_2O_3 hybrids

The catalytic reaction was performed in the PBS buffer (0.2 M, pH 7.4) with 100 mM hydrogen peroxide as substrate and GO-Fe_2O_3 hybrids as catalyst. The generated oxygen in the reaction system catalyzed by GO-Fe_2O_3 hybrids, Fe_2O_3 nanoparticles and GO were measured and compared by a multi-parameter analyzer.

2.5. The Michaelis-Menten kinetic analysis

Steady-state kinetic assays were conducted using a microplate reader at 25 °C. The reaction system was NaAc-HAc buffer (0.2 M, pH 3.6) in a 96-well plate containing H_2O_2 and TMB (or ABTS) as substrates and GO-Fe_2O_3 hybrids or Fe_2O_3 nanoparticles as peroxidase mimetics. The kinetic assay of TMB (or ABTS) as the substrate

was performed by adding 32 μL 30% H_2O_2 and different amounts (1, 2, 4, 6, 8, 10, 12 μL) of TMB solution (5 mg/mL dissolved in DMSO) or ABTS solution (10 mg/mL, dissolved in deionized water). The kinetic assay of H_2O_2 as the substrate was performed by adding 10 μL TMB and different amounts (2, 4, 6, 8, 16, 32, 64 μL) of 30% H_2O_2 solution, or 10 μL ABTS and different amounts (2, 4, 6, 8, 16, 32, 64 μL) of 3% H_2O_2 solution. All the reactions were monitored at 650 nm for TMB or 405 nm for ABTS using the microplate reader. Catalytic parameters were determined by fitting the absorbance data to the Michaelis–Menten as Eq. (3).

$$v = \frac{v_{max}[S]}{K_m + [S]} \quad (3)$$

The Michaelis–Menten equation describes the relationship between the rates of substrate conversion by the enzyme and the concentration of the substrate. In this equation, v is the rate of conversion, v_{max} is the maximum rate of conversion, [S] is the substrate concentration, and K_m is the Michaelis constant. The Michaelis constant is equivalent to the substrate concentration at which the rate of conversion is half of v_{max} and K_m approximates the affinity of the enzyme for the substrate.

2.6. pH, temperature and GO-Fe_2O_3 hybrid concentration dependence

The colorimetric reaction was carried under different pH, temperature and GO-Fe_2O_3 hybrids or Fe_2O_3 nanopartciles concentration. The pH was from 2 to 11; the temperature increased gradually from 4 °C to 70 °C; and the catalyst concentration was from 0.03 mM to 0.25 mM. These muti-parameter dependences were recorded through the absorbance value of the color metric reaction system using a microplate reader.

2.7. ESR assay

The electron spin resonance (ESR) technique was used to identify the reactive radicals (•OH, O_2^{-}• and TMB radicals) in the enzyme-like catalytic reaction process. TMB radicals could be directly detected because of its intensive ESR signal. But due to the very short lifetime and low steady-state concentration, •OH and O_2^{-}•/HO_2• could not be directly detected by ESR. Here we employed the spin-trapping ESR technique, in which a diamagnetic nitrone spin trapping agent was used to react with the radicals, forming a stable spin adduct that could be identified via ESR. In the experiments, the ESR signal of the spin adduct in the acidic reaction system (NaAc-HAc buffer, pH 3.6) was recorded at different time to investigate the mechanism of peroxidase-like activity; to study the mechanism of catalase-like activity, in PBS buffer, H_2O_2 was pre-irradiated with UV-light to generate free radicals, and 100 mM DMPO was added to form the stable DMPO-•OH and DMPO-O_2^{-}•/HO_2• signal, then different concentration of GO-Fe_2O_3 hybrids were added into the system to decompose H_2O_2, thus leading to the signal intensity decrease of reactive radicals.

2.8. Test of degradation RhB activity of GO-Fe_2O_3 hybrids

The degrade reaction was carried out in the hydrochloric acid (1.2 mL, pH 3) and RhB aqueous solution(500 μL, 0.02 mg/mL) with100 μL hydrogen peroxide, while GO-Fe_2O_3 hybrids (500 μL, 0.85 mM) (Fe_2O_3 nanoparticles, GO) was used as catalyst. The degrade reaction was continued for 5 h in a thermostat oscillator at 35 °C. After centrifugation, the absorbance values (Abs) of the supernatant liquid was tested with the ultraviolet visible absorption spectra to compare their degradation effect.

Furthermore, the degradation of RhB by GO-Fe_2O_3 hybrids in the presence of H_2O_2 was investigated under different conditions. The requirement of H_2O_2 and GO-Fe_2O_3 hybrids in degrading RhB was investigated. The reaction times were adjusted from 0 to 9 h, pH was from 2 to 9 and the temperature increased gradually from 4 °C to 80 °C. The degradation of 0.2 μg/mL RhB by different concentration of hydrogen peroxide (0 mM, 62.5 mM, 125 mM, 250 mM, 500 mM, 750 mM, 1 M, 1.5 M, 2 M, 3 M, 4.5 M, 6 M) was conducted, and experiments were carried out to study the optimal content of GO-Fe_2O_3 hybrids (0 mM, 0.08 mM, 0.17 mM, 0.25 mM, 0.34 mM, 0.51 mM, 0.68 mM, 0.85 mM, 1.02 mM, 1.18 mM) in the reaction system. The suspension were centrifuged to get the supernatant for analysis.

2.9. Characterization

A JEOL JEM-2100 transmission electron microscope (TEM) was employed to observe the morphology of the GO-Fe_2O_3 hybrids. Agilent PicoPlus Atomic force microscopy (AFM) was used to measure the thickness of the GO-Fe_2O_3 hybrids. Ultraviolet visible (UV–vis) absorption spectra were measured on an UV–vis-NIR spectrophotometer (Shimadzu UV-3600, Japan). The magnetism of the hybrids and Fe_2O_3 nanoparticles was characterized by a vibrating sample magnetometer (VSM, Lakeshore VSM 7407, USA). The peroxidase-like activity and the Michaelis constants were recorded on a bio-rad 680 microplate reader. The catalase-like activity was measured according to the amount of oxygen generated on a Multi-Parameter Analyzer (DZS-708, Cany Precision Instruments Co., Ltd). The mechanism of peroxidase-like and catalase-like activity was studied by Electron Spin Resonance (ESR) (EMX-10/12, Bruker, Germany).

3. Results and discussion

3.1. Preparation and characterization of GO-Fe_2O_3 hybrids

Fig. 1 and Fig. 2 show the typical TEM and AFM images of the obtained hybrids. It can be seen that Fe_2O_3 nanoparticles (average 21.3 nm in diameter) were adsorbed around the edge and the goffers of GO sheet (average 1.21 nm in height). From TEM image, it can be observed that the size and morphology of Fe_2O_3 nanoparticles after reacting with GO sheet almost remained the same with individual Fe_2O_3 nanoparticles before reaction, which indicated that the synthesis process of the hybrids did not change the size and morphology of Fe_2O_3 nanoparticles. UV–vis absorption spectra of the hybrids presented GO's characteristic peak at 224 nm corresponding to the $\pi \rightarrow \pi^*$ transitions of aromatic C—C bonds [34] and the broad absorption of Fe_2O_3 nanoparticles in the range of 200–500 nm (Fig. S1), resulting from the formation of the hybrids. The GO-Fe_2O_3 hybrids also remain most magnetism of Fe_2O_3 nanoparticle (about 97.3%) (Fig. S2). The magnetic properties of GO-Fe_2O_3 hybrids which supplied by Fe_2O_3 nanoparticles is useful in their purification by magnetic separation.

3.2. The peroxidase-like activity of the GO-Fe_2O_3 hybrids

The peroxidase-like activity of GO-hybrids was monitored through a colormetric reaction using TMB or ABTS as substrates in the presence of H_2O_2. Fig. 3 shows the time-dependent absorbance changes with the hybrids, Fe_2O_3 nanoparticles and GO as catalysts, respectively. The absorbance value of substrate oxidation products represents the relative peroxidase-like activity. At the same iron concentration, GO-Fe_2O_3 hybrids exhibit much stronger peroxidase-like activity compared with the Fe_2O_3 nanoparticles, while GO itself shows very low peroxidase-like activity, with TMB as substrate (Fig. 3) or ABTS as substrate (Fig. S3). This means that the peroxidase-like activity is greatly enhanced by assembling Fe_2O_3 nanoparticles onto GO sheet, where the Fe_2O_3 nanoparticles

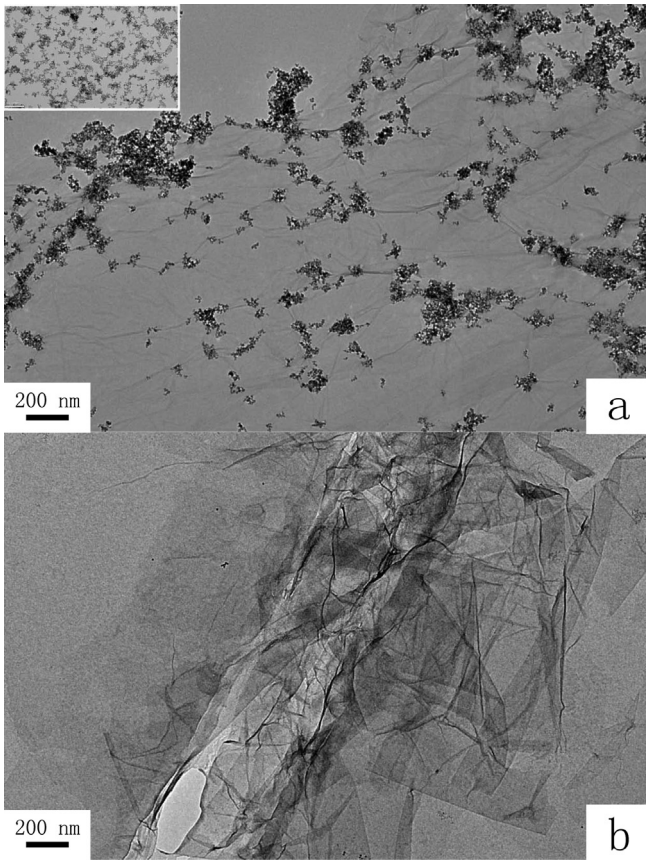

Fig. 1. TEM images of (a) GO-Fe_2O_3 hybrids and (b) GO sheet, the inset is TEM image of Fe_2O_3 nanoparticles.

Table 1
Comparison of the kinetic parameters of GO-Fe_2O_3 hybrids and Fe_2O_3 nanoparticles. K_m is the Michaelis constant and v_{max} is the maximal reaction velocity.

Catalyst	Substrate	K_m (mM)	v_{max} (Ms^{-1})
hybrids	TMB	0.118	5.38×10^{-8}
hybrids	H_2O_2(TMB)	305	1.01×10^{-7}
Fe_2O_3 nanoparticles	TMB	0.439	4.23×10^{-8}
Fe_2O_3 nanoparticles	H_2O_2(TMB)	120	1.72×10^{-7}
hybrids	ABTS	0.153	2.50×10^{-8}
hybrids	H_2O_2(ABTS)	13.8	2.43×10^{-8}
Fe_2O_3 nanoparticles	ABTS	0.258	1.46×10^{-8}
Fe_2O_3 nanoparticles	H_2O_2(ABTS)	11.3	2.17×10^{-8}

act as enzyme-like catalytic centers and GO may play an important role in the enhancement of the catalytic activity.

3.3. Steady-state enzyme kinetics

The peroxidase-like activity of the GO-Fe_2O_3 hybrids was also investigated by determining the apparent steady-state kinetic parameters of the catalytic reaction. With the suitable range of H_2O_2 concentrations, typical Michaelis-Menten curves were observed for TMB (Fig. S4) and ABTS (Fig. S5). The data were fitted to the Michaelis-Menten model to obtain the parameters (Table 1).

The apparent K_m values of the GO-Fe_2O_3 hybrids with both TMB and ABTS as the substrate were lower than that of the Fe_2O_3 nanoparticles alone, suggesting that the GO-Fe_2O_3 hybrids have a higher affinity to the substrate than Fe_2O_3 nanoparticles. This is likely due to the existence of strong interaction between the substrates and GO [20,35]. From the structure of TMB and ABTS, a π-π interaction could be considered as a dominant role to facilitate the substrate adsorption and enrichment around the Fe_2O_3 nanopar-

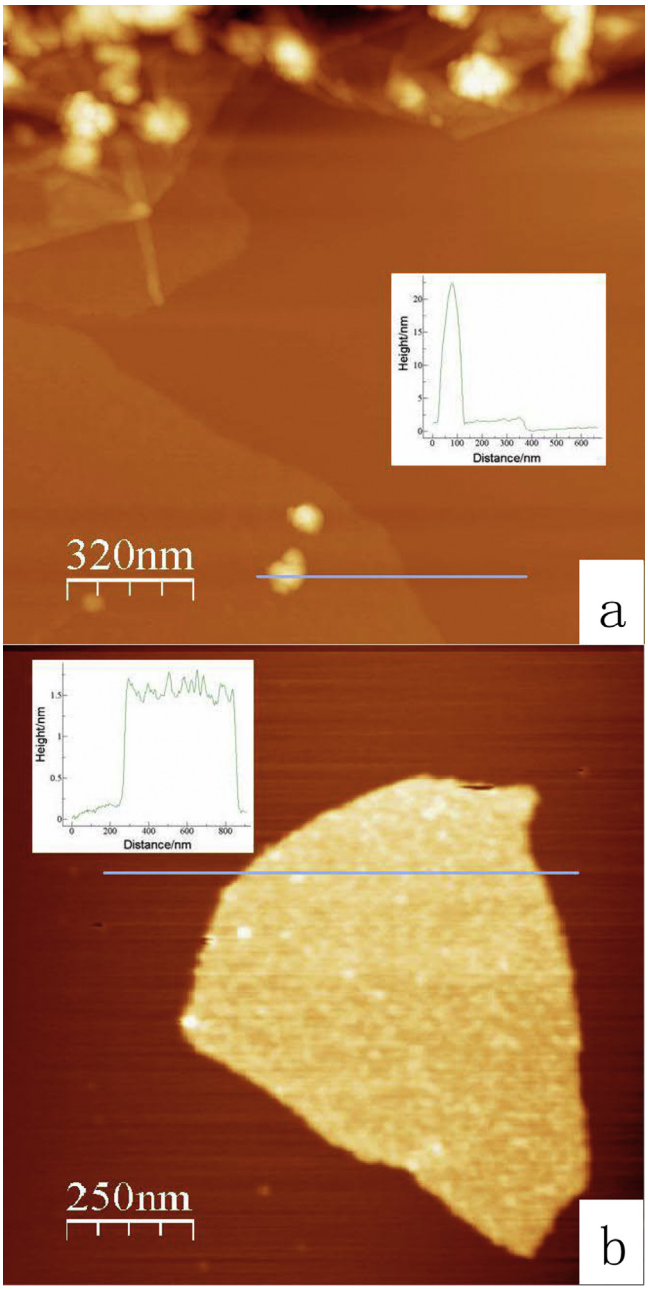

Fig. 2. AFM images of (a) GO-Fe_2O_3 hybrids and (b) GO sheet.

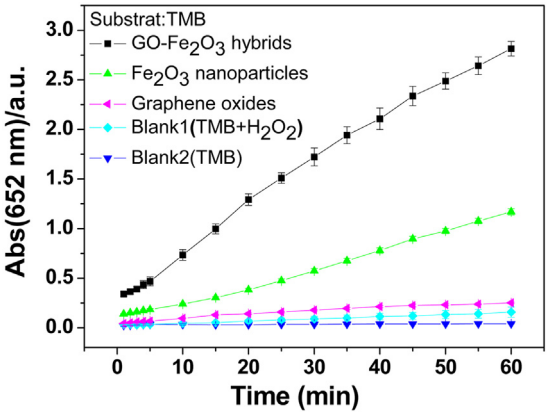

Fig. 3. The time-dependent absorbance changes at 652 nm in the presence of H_2O_2 with TMB as substrate.

ticles assembled on GO sheets. As a result, the GO-Fe_2O_3 hybrids exhibited larger v_{max} than that of Fe_2O_3 nanoparticles. Besides the adsorption effect, there could also exist enhanced electron transfer between catalytic centers and substrates through GO sheets. This enhanced electron transfer between TMB and H_2O_2 was also reported in previous catalytic reaction using individual GO as catalyst [20]. For TMB, the K_m values showed more obvious decrease from 0.439 mM (Fe_2O_3 nanoparticles) to 0.118 mM (hybrids) than that for ABTS (from 0.258 mM to 0.153 mM), resulting from the different substrate affinity of the Fe_2O_3 nanoparticles as well as the different adsorption capacity of substrates on GO sheets. According to the literature [13], horseradish peroxidase (HRP) possesses K_m values of 0.434 mM and 3.70 mM with TMB and H_2O_2 as substrates, respectively. In contrast, the K_m value of the GO-Fe_2O_3 hybrids with TMB as substrate is about four times lower than HRP, suggesting that the hybrids have a higher affinity for TMB than HRP. However, the affinity does not improve for the GO-Fe_2O_3 hybrids compared with HRP for H_2O_2. The large K_m values for H_2O_2 mean that a higher concentration of H_2O_2 was required to reach the v_{max} for both the hybrids and Fe_2O_3 nanoparticles. In addition, the K_m values for H_2O_2 seem to be dependent on another substrate, which becomes dramatically small taking ABTS as substrate.

3.4. The pH, temperature and catalyst concentration dependence

The catalytic activity of the GO-Fe_2O_3 hybrids is supposed to be dependent on pH, temperature and catalyst concentration like individual Fe_2O_3 nanoparticles [14]. We measured the peroxidase-like activity of the GO-Fe_2O_3 hybrids while varying the pH from 2 to 12, the temperature from 4 °C to 70 °C, the catalyst concentration from 0 to 0.248 mM and compared the results with the activity shown in the Fe_2O_3 nanoparticles over the same range of parameters. First of all, GO-Fe_2O_3 hybrids concentration dependence of the peroxidase-like activity was studied. There was a linear absorbance increase with a correlation coefficient of 0.992 as a function of hybrids concentration, indicating that the hybrids as-prepared can be used as a suitable mimic enzyme (Fig. S6a). The optimal pH and temperature were approximately 3.6 and 45 °C, which are very similar to the values for Fe_2O_3 nanoparticles (Fig. S6b–d). Considering the facile condition of the reaction, we adopted pH 3.6 and 25 °C (room temperature) as standard conditions for subsequent analysis of GO-Fe_2O_3 hybrids' peroxidase-like activity.

3.5. The high adsorption capacity of GO

The high substrate adsorption capacity of GO sheets was likely an important factor to the strong enzyme mimetic activity of the GO-Fe_2O_3 hybrids. Similar adsorption between GO and dye or drug molecules, such as phthalocyanine, doxorubicin and camptothecin, has already been reported [36–39]. In order to study it, TMB was treated with and without GO. The characteristic peak of TMB was observed at 285 nm in UV–vis absorption spectra. The absorption spectra of GO/TMB mixture was recorded every 30 min for 4 h. During the treating time, the absorption spectra appeared a more rapid intensity decrease along with red-shifts (2.5 nm) (Fig. S7a). This implied the occurrence of strong π-π interaction between GO and TMB molecules similar with previous reports [20]. In contrast, the absorption peak intensity varies slowly for TMB without treatment of GO, possibly due to intermolecular interaction of TMB in the NaAc-HAc buffer (Fig. S7b).

3.6. Free radical detection

Furthermore, ESR assay was used to detect the radicals generated through the Fenton reaction or quasi-Fenton reaction as written in (1) and (2) with GO-Fe_2O_3 hybrids as catalyst. Firstly,

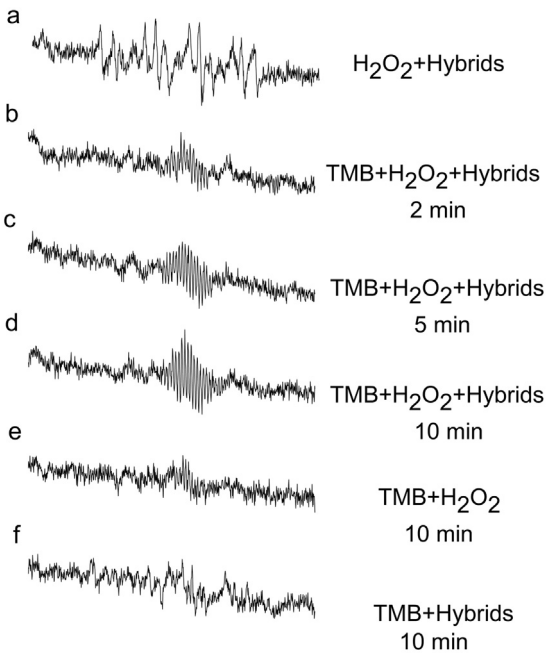

Fig. 4. DMPO spin-trapping ESR spectra of TMB-H_2O_2-hybrids system.

the produced free radical from H_2O_2 as •OH and O_2^{-}•/HO_2• radicals were identified by the addition of the spin-trapping agent DMPO. In the catalytic reaction system, when TMB was not added, both the typical signature of DMPO-•OH and DMPO-O_2^{-}•/HO_2• appeared (Fig. 4a), indicating the presence of •OH and O_2^{-}•/HO_2• as reaction intermedia [40]. After TMB was added to form the TMB-H_2O_2-hybrids system, •OH and O_2^{-}•/HO_2• signals were suppressed rapidly and a new radical signature was generated, which was identified as the TMB radical according to the previous report [41], and the intensity of the signature increased with the reaction time (Fig. 4b–d). It implied that ·OH and O_2^{-}•/HO_2• generated from the catalytic reaction intended to be consumed by TMB and leaded to the oxidation of TMB. Meanwhile, without GO-Fe_2O_3 hybrids as catalyst, such ESR signal was not observed in control experiment (Fig. 4e), which indicated that GO-Fe_2O_3 hybrids could really accelerate the reaction velocity greatly. When H_2O_2 was not added into the system, there were no obvious free radicals to be observed (Fig. 4f). In order to further identify •OH and O_2^{-}•/HO_2•, two distinguished kinds of radical inhibitors were introduced to the TMB-H_2O_2-hybrids system. When 10 mM p-benzoquinone was added to act as the O_2^{-}•/HO_2• radical quencher [42], the TMB oxidation was greatly suppressed (Fig. S8). Meanwhile, the addition of 1 M t-butyl alcohol, which is considered as a well-known ·OH radical scavenge [43], had similar effect on the TMB oxidation. However, when the concentration of t-butyl alcohol was decreased to the same concentration as p-benzoquinone, there was little inhibition effect. Therefore, O_2^{-}•/HO_2• radicals exhibited a much stronger effect than •OH radicals in the TMB oxidation with H_2O_2 as oxidant and GO-Fe_2O_3 hybrids as catalyst. These evidences demonstrated that although both •OH and O_2^{-}•/HO_2• radicals were formed in GO-Fe_2O_3 hybrids participating catalytic reaction, the O_2^{-}•/HO_2• radicals were main reactive radicals, that is, the quasi-Fenton reaction started from ferric ion (Eq. (2)) was the main mechanism, of which the contribution was enlarged by GO due to its enhanced substrate enrichment ability and electron transfer capacity. The contribution of –OH radicals was relatively small, attributed to the lack of Fe^{2+} in Fe_2O_3 nanoparticles which contributed the catalytic reaction through Fenton reaction (Eq. (1)).

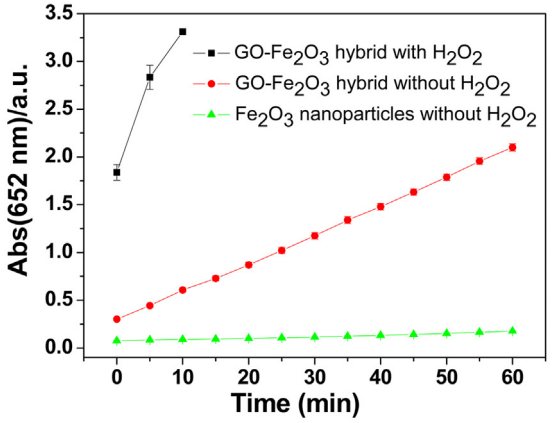

Fig. 5. The oxidation capacity of the GO-Fe_2O_3 hybrids and Fe_2O_3 nanoparticles in the absence of H_2O_2. The substrate oxidation reaction in the presence of H_2O_2 was used as contrast.

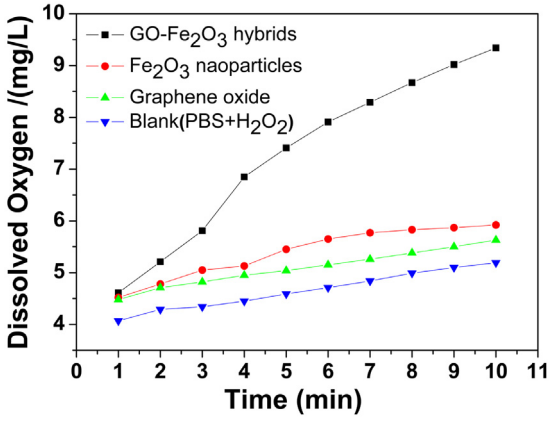

Fig. 6. The oxygen generated with GO-Fe_2O_3 hybrids, Fe_2O_3 nanoparticles and GO as mimetic catalases.

3.7. The intrinsic oxidation capacity of ferric ion enhanced by GO

In the TMB-hybrids-H_2O_2 system, hybrids were considered as catalyst and H_2O_2 plays the role of oxidant. However, ferric ions in the hybrids may possess some intrinsic oxidation capacity, whether the hybrids could oxidize TMB in the absence of H_2O_2 need to be studied. In order to prove this, the reaction was carried out in the absence of H_2O_2. It is observed that the substrate could also be oxidized by GO-Fe_2O_3 hybrids. Different from the reaction carried out in the presence of H_2O_2, the absorbance value increased more slowly (Fig. 5), which means ferric ion possesses the oxidation ability but is limited. When H_2O_2 was added into the redox reaction system, the effect of ferric ion itself could hardly be observed because the oxidation ability of H_2O_2 or newly generated •OH and O_2^{-}• was much stronger than that of ferric ion, the substrate intended to be oxidized by H_2O_2 or free radicals before ferric ion. In this experiment, GO in the hybrids could enrich substrates and accelerate the electron transport in the reaction system, which was reported by similar research [28,44,45], so the intrinsic oxidation ability of ferric ion could be enhanced relatively.

Based on the above discussions, we assume one likely catalytic mechanism: Fe_2O_3 nanoparticles with a high concentration on GO sheets act as catalytic centers, and the substrates such as TMB are adsorbed and enriched on the surface of GO sheets and around Fe_2O_3 nanoparticles. When H_2O_2 is added, the catalytic centers reacts with H_2O_2 to generate O_2^{-}•/HO_2• (main) and •OH, at this time, these free radicals oxidize the substrates to form TMB oxidation products (TMB^{ox}), where the enhanced electron transfer capacity of GO sheets plays possibly an important role in accelerating catalytic reaction velocity.

3.8. The catalase-like activity of the GO-Fe_2O_3 hybrids

As described above, with the increase of pH from 3 to 11, the absorbance value was decreased, which meant the peroxidase-like activity of the hybrids was inhibited. Interestingly, in the alkaline and neutral buffer, bubbles were observed (Fig. S9), which were considered as oxygen, and the color reaction was suppressed. It implied that GO-Fe_2O_3 hybrids we prepared might possess catalase-like activity rather than peroxidase-like activity in alkaline and neutral buffer.

The generated oxygen was identified using an oxygen electrode installed on a Multi-Parameter Analyzer and was monitored through real-time detection of the amount of dissolved oxygen in the reaction system, where GO-Fe_2O_3 hybrids, Fe_2O_3 nanoparticles and GO sheet were used as catalyst respectively to compare their activities (Fig. 6). Within 10 min, the dissolved oxygen in the reaction system was increased to 9.34 mg/mL with the hybrids as catalyst, much more than that with Fe_2O_3 nanoparticles or GO alone. It implied the enhanced catalase-like activity of the GO-Fe_2O_3 hybrids.

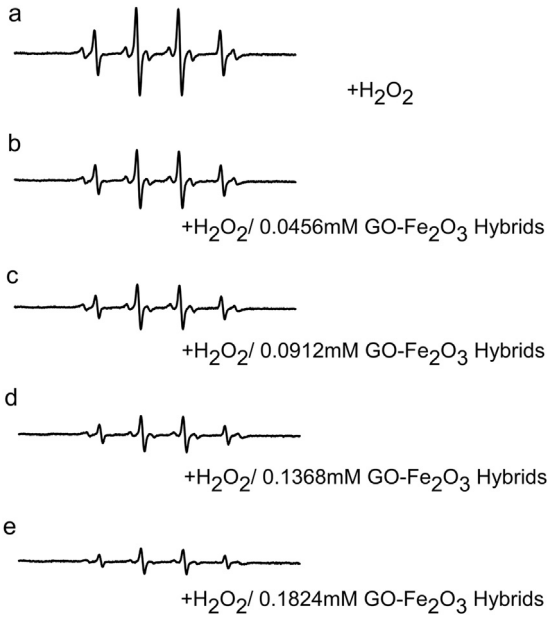

Fig. 7. The effects of (a) 0 mM (b) 0.0456 mM (c) 0.0912 mM (d) 0.1368 mM (e) 0.1824 mM GO- Fe_2O_3 hybrids on hydroxyl radical formation.

The ESR detection was also used to monitor the H_2O_2 decomposition process, this method was often adopted in previous reports [46,47]. First, the hydrogen peroxide was exposed under the UV irradiation to generate •OH radical. With the spin-trapping agent DMPO, the four-fold characteristic peaks with an intensity ratio of 1:2:2:1 (the typical DMPO-•OH adduct) was observed (Fig. 7a). Then different amount of GO-Fe_2O_3 hybrids were added into the system, the DMPO-•OH signal was decreased in a dose dependent fashion (Fig. 7b–e). It demonstrated that GO-Fe_2O_3 hybrids could act as a catalase mimetic to catalyze H_2O_2 decomposition in neutral environment and thus the •OH radical ESR signal was suppressed.

Based on the above results, the possible mechanism of the hybrids' catalase-like activity could be written as (4),

$$2H_2O_2 \xrightarrow{GO-Fe_2O_3\,hybrids} 2H_2O + O_2 \uparrow \quad (4)$$

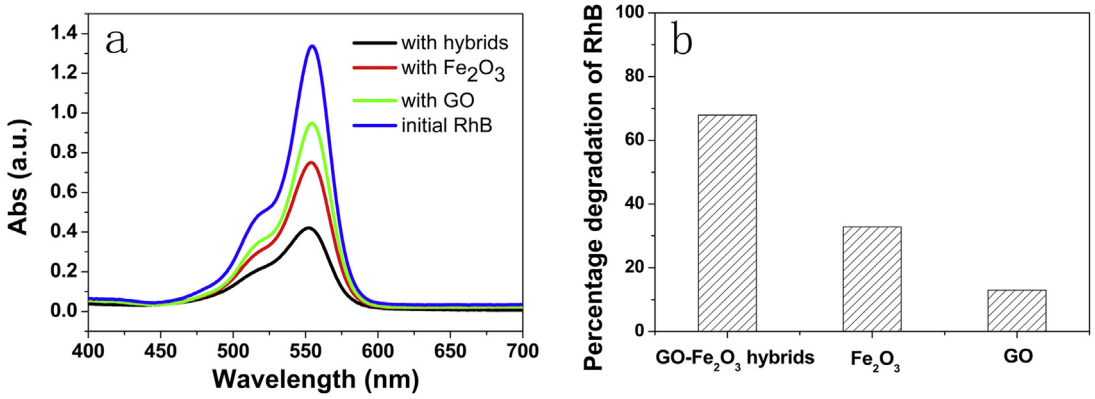

Fig. 8. UV–vis spectra (A) and degradation rate (B) of RhB after treatment with GO-Fe_2O_3 hybrids, Fe_2O_3 nanoparticles and GO.

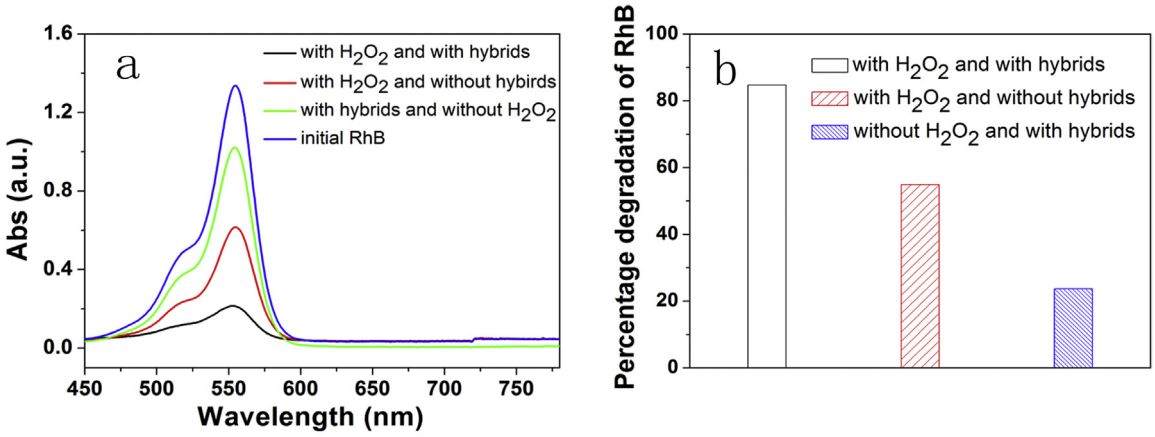

Fig. 9. UV–vis spectra (A) and degradation rate (B) of RhB after treatment with GO-Fe_2O_3hybrids and different H_2O_2 concentrations.

Where H_2O_2 was decomposed and the oxygen is generated. Similar mechanism of H_2O_2 decomposition had been reported in previous literature [48,49] using Fe^{3+} ions or granular goethite (α-FeOOH) particles as catalysts, and the mechanism could be attributed to Fe^{3+}-initiated $O_2^{-\bullet}/HO_2^{\bullet}$ radical generation and subsequent O_2 formation.

3.9. The degradation RhB activity of GO-Fe_2O_3 hybrids

The degradation RhB activity byGO-Fe_2O_3 hybrids was investigated in the presence of hydrogen peroxide. Compared with Fe_2O_3 nanoparticles and GO, GO-Fe_2O_3 hybrids have enhanced degradation activity of RhB. The intensity of the finger print peak at 552 nm of initial RhB declines greatly after treatment with GO-Fe_2O_3 hybrids (Fig. 8A), with the absorbance value reduces from 1.31 to 0.42. The results demonstrated that 67.9% of degradation of RhB took place in GO-Fe_2O_3 hybrids group, whereas in the Fe_2O_3 nanoparticles and GO groups, the percentages degradation of RhB were 32.8% and 13.0%, respectively, as shown in Fig. 8B. It is certain that GO-Fe_2O_3 hybrids reflect the better degradation Rhb ability than that of Fe_2O_3 nanoparticles and GO. Just as the catalyze activity on TMB and ABTS, GO in the GO-Fe_2O_3 hybrids acts as an amplifier in accelerating catalytic reaction velocity of Fe_2O_3 nanoparticles.

The requirement of H_2O_2 and GO-Fe_2O_3 hybrids in degrading RhB was studied. It can be seen from Fig. S10, the degradation rate of RhB has important significance only in the presence of both GO-Fe_2O_3 hybrids and H_2O_2. It is reduced remarkably while missing one of them. The results prove the degradation mechanism of this method, where GO-Fe_2O_3 hybrids play key role in strengthening the capacity to oxidize RhB by H_2O_2.

3.10. The optimum for degrading RhB by GO-Fe_2O_3 hybrids

To enhance the degradation rate of RhB, it is necessary to investigated influence of time, pH and temperature on the degradation activity of the GO-Fe_2O_3 hybrids. We measured the degradation activity of GO-Fe_2O_3 hybrids while varying the time from 0 to 9 h, pH from 2 to 12, the temperature from 4 to 80 °C and compared the results with the same range of other parameters. The degradation rate of RhB was increased with prolonging the reaction time and maintain a steady state between 7 h and 9 h (Fig. S11a). The highest degradation rate of RhB appears at pH 3 (Fig. S11b), which is consistent with the pH of TMB and ABTS catalytic oxidation by GO-Fe_2O_3 hybrids. The degradation effect shows a positive correlation with temperature (Fig. S11c). While the temperature rise to 60 °C, the remain RhB in the reaction system reduces from 100% to 5%.

The enhancement in degradation of RhB by the addition of H_2O_2 increases the concentration of hydroxyl radical and it could act as an alternative electron acceptor to oxygen. The results shown in Fig. S11d demonstrated that the degradation rate of RhB was increased when the H_2O_2 concentration was increased from 0 M to 3 M. However, the degradation ability of RhB drops with the H_2O_2 concentration is greater than 3 M. It means that the catalysis of GO-Fe_2O_3 hybrids can be stimulated in a certain range of H_2O_2 concentration in the reaction system. High H_2O_2 concentration inhibit the catalysis ability of GO-Fe_2O_3 hybrids, which is consisted with the mimic enzyme activity of hybrids.

Whether the more amount of GO-Fe_2O_3 hybrids the better the degradation ability in the reaction system is investigated. Degradation rate of RhB increases with the increasing of additive hybirds concentration, and then decreases when it is greater than 0.85 mM (Fig. S12). Results demonstrated that the optimum conditions for higher percentage degradation of RhB were obtained with H_2O_2 concentration (3 M), pH = 3, temperation of 60 °C, reaction time of 7 hand GO-Fe_2O_3 hybrids dose of 0.85 mM (Fig. 9).

4. Conclusions

In summary, we have shown that GO-Fe_2O_3 hybrids combine the mimetic enzyme activity of Fe_2O_3 nanoparticles and the excellent characteristic of GO such as high adsorption capacity and rapid electron conduction. It has been demonstrated that the peroxidase-like activity of the GO-Fe_2O_3 hybrids is pH, temperature and hybrid concentration dependent and fits well with typical Michaelis–Menten kinetics. More importantly, we demonstrated that GO-Fe_2O_3 hybrids possess both peroxidase-like and catalase-like activities in different pH buffers. In acidic buffer, the GO-Fe_2O_3 hybrids are peroxidase mimetics and could catalyze H_2O_2 to generate ·OH and O_2^- to oxidize the substrates; meanwhile, in neutral and alkaline buffers, GO-Fe_2O_3 hybrids play the role of catalase mimetics and breakdown H_2O_2 to form oxygen. From this work, GO-Fe_2O_3 hybrids we prepared will exhibit great potential in the enrichment, magnetic separation and degradation of aromatic pollutants in the acidic condition. The relevant work is under study. And GO-Fe_2O_3 hybrids can be used to catalyze the oxidize RhB from waste water by H_2O_2, which is meaningful in waste water treatment.

Conflict of interests

The authors declare that there is no conflict of interests regarding the publication of this paper.

Acknowledgements

This research was supported by the National Key Basic Research Program of China (973 program No. CB733800), the National Natural Science Foundation of China (No. 81571806), the Jiangsu Provincial Special Program of Medical Science (No. BL2013029), the Jiangsu Provincial Technical Innovation Fund for Scientific and Technological Enterprises (No. SBC201310643), and the National High Technology Research and Development Program of China (No. 2013AA032205). Collaborative Innovation Center of Suzhou Nano Science and Technology.

Appendix A. Supplementary data

Supplementary data associated with this article can be found, in the online version, at http://dx.doi.org/10.1016/j.colsurfa.2016.07.037.

References

[1] X. Zhang, S. Gong, Y. Zhang, T. Yang, C. Wang, N. Gu, Prussian blue modified iron oxide magnetic nanoparticles and their high peroxidase-like activity, J. Mater. Chem. 20 (2010) 5110.
[2] J.M. Perez, F.J. Simeone, A. Tsourkas, L. Josephson, R. Weissleder, Peroxidase substrate nanosensors for MR imaging, Nano Lett. 4 (2004) 119–122.
[3] Y. Wu, M. Song, Z. Xin, X. Zhang, Y. Zhang, C. Wang, S. Li, N. Gu, Ultra-small particles of iron oxide as peroxidase for immunohistochemical detection, Nanotechnology 22 (2011) 225703.
[4] J. Cheng, B.A. Teply, S.Y. Jeong, C.H. Yim, D. Ho, I. Sherifi, S. Jon, O.C. Farokhzad, A. Khademhosseini, R.S. Langer, Magnetically responsive polymeric microparticles for oral delivery of protein drugs, Pharm. Res. 23 (2006) 557–564.
[5] Y. Yang, J.S. Jiang, B. Du, Z.F. Gan, M. Qian, P. Zhang, Preparation and properties of a novel drug delivery system with both magnetic and biomolecular targeting, J. Mater. Sci. Mater. Med. 20 (2009) 301–307.
[6] M.L. Gou, Z.Y. Qian, H. Wang, Y.B. Tang, M.J. Huang, B. Kan, Y.J. Wen, M. Dai, X.Y. Li, C.Y. Gong, Preparation and characterization of magnetic poly (ε-caprolactone)-poly (ethylene glycol)-poly (ε-caprolactone) microspheres, J. Mater. Sci. Mater. Med. 19 (2008) 1033–1041.
[7] M.L. Matteucci, G. Anyarambhatla, G. Rosner, C. Azuma, P.E. Fisher, M.W. Dewhirst, D. Needham, D.E. Thrall, Hyperthermia increases accumulation of technetium-99m-labeled liposomes in feline sarcomas, Clin. Cancer Res. 6 (2000) 3748–3755.
[8] I.J. Majoros, A. Myc, T. Thomas, C.B. Mehta, J.R. Baker, PAMAM dendrimer-based multifunctional conjugate for cancer therapy: synthesis, characterization, and functionality, Biomacromolecules 7 (2006) 572–579.
[9] M. Brähler, R. Georgieva, N. Buske, A. Müller, S. Müller, J. Pinkernelle, U. Teichgräber, A.A. Voigt, H. Bäumler, Magnetite-Loaded carrier erythrocytes as contrast agents for magnetic resonance imaging, Nano Lett. 6 (2006) 2505–2509.
[10] M.C. Denis, U. Mahmood, C. Benoist, D. Mathis, R. Weissleder, Imaging inflammation of the pancreatic islets in type 1 diabetes, PNAS 101 (2004) 12634–12639.
[11] C. Burtea, S. Laurent, A. Roch, L.V. Elst, R.N. Muller, C-MALISA (cellular magnetic-linked immunosorbent assay), a new application of cellular ELISA for MRI, J. Inorg. Biochem. 99 (2005) 1135–1144.
[12] S. Boutry, S. Laurent, L.V. Elst, R.N. Muller, Specific E-selectin targeting with a superparamagnetic MRI contrast agent, Contrast Media Mol. Imaging 1 (2006) 15–22.
[13] C.K. Duesterberg, S.E. Mylon, W.T. David, pH effects on iron-catalyzed oxidation using Fenton's reagent, Environ. Sci. Technol. 42 (2008) 8522–8527.
[14] L. Gao, J. Zhuang, L. Nie, J. Zhang, Y. Zhang, N. Gu, T. Wang, J. Feng, D. Yang, S. Perrett, Intrinsic peroxidase-like activity of ferromagnetic nanoparticles, Nat. Nanotechnol. 2 (2007) 577–583.
[15] Y. Zhuo, P. Yuan, R. Yuan, Y. Chai, C. Hong, Bienzyme functionalized three-layer composite magnetic nanoparticles for electrochemical immunosensors, Biomaterials 30 (2009) 2284–2290.
[16] L. Gao, J. Wu, S. Lyle, K. Zehr, L. Cao, D. Gao, Magnetite nanoparticle-linked immunosorbent assay, J. Phys. Chem. C 112 (2008) 17357–17361.
[17] Y.S. Kang, S. Risbud, J.F. Rabolt, P. Stroeve, Synthesis and characterization of nanometer-size Fe_3O_4 and γ-Fe_2O_3 particles, Chem. Mater. 8 (1996) 2209–2211.
[18] Y. Lan, X. Li, G. Li, Y. Luo, Sol–gel method to prepare graphene/Fe_2O_3 aerogel and its catalytic application for the thermal decomposition of ammonium perchlorate, J. Nanopart. Res 17 (2015) 1–9.
[19] L. Chen, B. Wei, X. Zhang, C. Li, Bifunctional graphene/γ-Fe_2O_3 hybrid aerogels with double nanocrystalline networks for enzyme immobilization, Small 9 (2013) 2331–2340.
[20] Y. Song, K. Qu, C. Zhao, J. Ren, X. Qu, Graphene oxide: intrinsic peroxidase catalytic activity and its application to glucose detection, Adv. Mater. 22 (2010) 2206–2210.
[21] C. Lee, X. Wei, J.W. Kysar, J. Hone, Measurement of the elastic properties and intrinsic strength of monolayer graphene, Science 321 (2008) 385–388.
[22] J. Chen, C. Jang, S. Xiao, M. Ishigami, M.S. Fuhrer, Intrinsic and extrinsic performance limits of graphene devices on SiO_2, Nat. Nanotechnol. 3 (2008) 206–209.
[23] R.F. Service, Materials science. Carbon sheets an atom thick give rise to graphene dreams, Science (New York, NY) 324 (2009) 875.
[24] A.A. Balandin, S. Ghosh, W. Bao, I. Calizo, D. Teweldebrhan, F. Miao, C.N. Lau, Superior thermal conductivity of single-layer graphene, Nano. Lett. 8 (2008) 902–907.
[25] P.V. Kamat, Graphene-Based nanoassemblies for energy conversion, J. Phys. Chem. Lett. 2 (2011) 242–251.
[26] W. Graeme, S. Brian, P.V. Kamat, TiO2-graphene nanocomposites. UV-assisted photocatalytic reduction of graphene oxide, ACS Nano 2 (2008) 1487–1491.
[27] R. Kou, Y. Shao, D. Wang, M.H. Engelhard, J.H. Kwak, J. Wang, V.V. Viswanathan, C. Wang, Y. Lin, Y. Wang, Enhanced activity and stability of Pt catalysts on functionalized graphene sheets for electrocatalytic oxygen reduction, Electrochem. Commun. 11 (2009) 954–957.
[28] Y. Fu, X. Wang, Magnetically separable $ZnFe_2O_4$—graphene catalyst and its high photocatalytic performance under visible light irradiation, Ind. Eng. Chem. Res. 50 (2011) 7210–7218.
[29] B. Tian, C. Wang, S. Zhang, L. Feng, Z. Liu, Photothermally enhanced photodynamic therapy delivered by nano-graphene oxide, ACS Nano 5 (2011) 7000–7009.
[30] K. Yang, J. Wan, S. Zhang, B. Tian, Y. Zhang, Z. Liu, The influence of surface chemistry and size of nanoscale graphene oxide on photothermal therapy of cancer using ultra-low laser power, Biomaterials 33 (2012) 2206–2214.
[31] K. Yang, J. Wan, S. Zhang, Y. Zhang, S. Lee, Z. Liu, In vivo pharmacokinetics, long-term biodistribution, and toxicology of PEGylated graphene in mice, ACS Nano 5 (2010) 516–522.
[32] S. Zhang, X. Chen, C. Gu, Y. Zhang, J. Xu, Z. Bian, D. Yang, N. Gu, The effect of iron oxide magnetic nanoparticles on smooth muscle cells, Nanoscale Res. Lett. 4 (2009) 70–77.
[33] M. Ma, Y. Zhang, W. Yu, H. Shen, H. Zhang, N. Gu, Preparation and characterization of magnetite nanoparticles coated by amino silane, Colloids Surf. A 212 (2003) 219–226.

[34] F. He, J. Fan, D. Ma, L. Zhang, C. Leung, H.L. Chan, The attachment of Fe_3O_4 nanoparticles to graphene oxide by covalent bonding, Carbon 48 (2010) 3139–3144.
[35] C. Huang, C. Li, G. Shi, Graphene based catalysts, Energy Environ. Sci. 5 (2012) 8848–8868.
[36] X. Zhang, Y. Feng, S. Tang, W. Feng, Preparation of a graphene oxide–phthalocyanine hybrid through strong π-π interactions, Carbon 48 (2010) 211–216.
[37] L. Zhang, J. Xia, Q. Zhao, L. Liu, Z. Zhang, Functional graphene oxide as a nanocarrier for controlled loading and targeted delivery of mixed anticancer drugs, Small 6 (2010) 537–544.
[38] X. Sun, Z. Liu, K. Welsher, J.T. Robinson, A. Goodwin, S. Zaric, H. Dai, Nano-graphene oxide for cellular imaging and drug delivery, Nano Res. 1 (2008) 203–212.
[39] Z. Liu, J.T. Robinson, X. Sun, H. Dai, PEGylated nanographene oxide for delivery of water-insoluble cancer drugs, J. Am. Chem. Soc. 130 (2008) 10876–10877.
[40] N. Wang, L. Zhu, D. Wang, M. Wang, Z. Lin, H. Tang, Sono-assisted preparation of highly-efficient peroxidase-like Fe_3O_4 magnetic nanoparticles for catalytic removal of organic pollutants with H_2O_2, Ultrason. Sonochem. 17 (2010) 526–533.
[41] R. Palominos, J. Freer, M.A. Mondaca, H.D. Mansilla, Evidence for hole participation during the photocatalytic oxidation of the antibiotic flumequine, J. Photochem. Photobiol. A 193 (2008) 139–145.
[42] I. Gültekin, G. Tezcanli-Güyer, N.H. Ince, Sonochemical decay of C.I. acid orange 8: effects of CCl 4 and t-butyl alcohol, Ultrason. Sonochem. 16 (2009) 577–581.
[43] G. Borthiry, W.B. Antholine, J. Myers, C. Myers, Reduction of hexavalent chromium by human cytochrome b5: generation of hydroxyl radical and superoxide, Free Radic. Biol. Med. 42 (2007) 738–755.
[44] W. Aleksandra, P.V. Kamat, Reduced graphene oxide and porphyrin. An interactive affair in 2-D, ACS Nano 4 (2010) 6697–6706.
[45] B. Seger, P.V. Kamat, Electrocatalytically active graphene-Platinum nanocomposites. role of 2-D carbon support in PEM fuel cells, J. Phys. Chem. C 113 (2009) 7990–7995.
[46] J. Fan, J. Yin, B. Ning, X. Wu, Y. Hu, M. Ferrari, G.J. Anderson, J. Wei, Y. Zhao, G. Nie, Direct evidence for catalase and peroxidase activities of ferritin–platinum nanoparticles, Biomaterials 32 (2011) 1611–1618.
[47] W. He, Y. Liu, J. Yuan, J. Yin, X. Wu, X. Hu, K. Zhang, J. Liu, C. Chen, Y. Ji, Au@Pt nanostructures as oxidase and peroxidase mimetics for use in immunoassays, Biomaterials 32 (2011) 1139–1147.
[48] P. Acker, J. Bordas, Dysproteinemia and pulmonary tuberculosis in an African environment (Congo Brazzaville). Electrophoretic and immunoelectrophoretic study, Environ. Sci. Technol. 33 (1999) 2726–2732.
[49] S.S.L. And, D.G. Mirat, Catalytic decomposition of hydrogen peroxide on iron oxide: kinetics, mechanism, and implications, Environ. Sci. Technol. 32 (1998) 1417–1423.